Plant, Cell and Environment (2003) **26,** 231–244

Modelling the discrimination of $^{13}CO_2$ above and within a temperate broad-leaved forest canopy on hourly to seasonal time scales

D. D. BALDOCCHI[1] & D. R. BOWLING[2]

[1]*Ecosystem Science Division, Department of Environmental Science, Policy and Management, 151 Hilgard Hall, University of California, Berkeley, CA 94720, USA and* [2]*Department of Biology, 257 S 1400 East, University of Utah, Salt Lake City, UT 84112, USA*

ABSTRACT

Fluxes and concentrations of carbon dioxide and $^{13}CO_2$ provide information about ecosystem physiological processes and their response to environmental variation. The biophysical model, *CANOAK,* was adapted to compute concentration profiles and fluxes of $^{13}CO_2$ within and above a temperate deciduous forest (Walker Branch Watershed, Tennessee, USA). Modifications to the model are described and the ability of the new model (*CANISOTOPE*) to simulate concentration profiles of $^{13}CO_2$, its flux density across the canopy–atmosphere interface and leaf-level photosynthetic discrimination against $^{13}CO_2$ is demonstrated by comparison with field measurements. The model was used to investigate several aspects of carbon isotope exchange between a forest ecosystem and the atmosphere. During the 1998 growing season, the mean photosynthetic discrimination against $^{13}CO_2$, by the deciduous forest canopy (Δ_{canopy}), was computed to be 22·4‰, but it varied between 18 and 27‰. On a diurnal basis, the greatest discrimination occurred during the early morning and late afternoon. On a seasonal time scale, the greatest diurnal range in Δ_{canopy} occurred early and late in the growing season. Diurnal and seasonal variations in Δ_{canopy} resulted from a strong dependence of Δ_{canopy} on photosynthetically active radiation and vapour pressure deficit of air. Model calculations also revealed that the relationship between canopy-scale water use efficiency (CO_2 assimilation/transpiration) and Δ_{canopy} was positive due to complex feedbacks among fluxes, leaf temperature and vapour pressure deficit, a finding that is counter to what is predicted for leaves exposed to well-mixed environments.

Key-words: biogeochemistry; biosphere–atmosphere interactions; canopy photosynthesis; carbon isotopes; water use efficiency.

Correspondence: Dennis D. Baldocchi.
E-mail: Baldocchi@nature.berkeley.edu

INTRODUCTION

Stable isotopes act as tracers for studying flows of material through ecosystems and the atmosphere (Farquhar, Ehleringer & Hubick 1989; Ehleringer, Hall & Farquhar 1993; Flanagan & Ehleringer 1998; Yakir & Sternberg 2000). In practice, ecologists and biogeochemists use information on the stable carbon isotope content of air, plants and soil to provide information on: (1) plant water use efficiency (Farquhar & Richards 1984; Farquhar *et al*. 1988; Condon, Richards & Farquhar 1993; Hall, Ismail & Menendez 1993); (2) recycling of respired carbon dioxide within forests (Schleser & Jayasekera 1985; Sternberg 1989; Lloyd *et al*. 1996; Sternberg *et al*. 1997; Yakir & Sternberg 2000); (3) the partitioning of net ecosystem carbon exchange into its components, photosynthesis and respiration (Yakir & Wang 1996; Bowling, Monson & Tans 2001); (4) identifying and quantifying the distribution and contributions of C_3 and C_4 species to global primary productivity (Lloyd & Farquhar 1994; Ehleringer, Cerling & Helliker 1997; Sage, Wedin & Li 1999); and (5) the partitioning of CO_2 exchange between terrestrial biosphere and oceanic reservoirs in global carbon cycle models (Ciais *et al*. 1995; Fung *et al*. 1997).

Plant material and the CO_2 respired by plants or the decomposition of plant material are depleted in ^{13}C relative to that in the atmosphere. This depletion is due to discrimination against CO_2 molecules containing the heavier isotope, ^{13}C, when molecules diffuse across the laminar boundary layer of leaves and are carboxylated by the enzyme Rubisco during photosynthesis (Farquhar *et al*. 1989; O'Leary, Madhaven & Paneth 1992; O'Leary 1993; Lloyd & Farquhar 1994; Yakir & Sternberg 2000). Other discriminating processes include the hydration of CO_2, and the diffusion of CO_2 in aqueous solution (O'Leary 1993). The isotopic signature of respiring roots, soil microbes and leaves, on the other hand, differ from one another due to their unique turnover times (Flanagan & Ehleringer 1998). Each respiring carbon pool possesses a different isotopic content because the isotopic content of the atmospheric CO_2 fixed by the plants is decreasing with time; fossil fuel combustion is diluting the isotopic content of the atmo-

sphere because it is oxidizing organic compounds that are depleted in ^{13}C, due to their photosynthetic origin (Francey *et al*. 1995). Consequently, carbon in older pools generally contains more ^{13}C than carbon that was assimilated more recently. Other factors leading to variation in the ^{13}C content of respiration include selective degradation of various organic compounds by microbes, leaching of soluble organic components, and refixation of diffusively enriched CO_2 within the soil gas (Gleixner *et al*. 1998; Ehleringer, Buchmann & Flanagan 2000).

Isotopic mixing lines, called 'Keeling plots' (Keeling 1958), are used to quantify the carbon isotope composition of respiring sources, such as an ecosystem and soil (Flanagan *et al*. 1996; Buchmann & Ehleringer 1998; Yakir & Sternberg 2000; Bowling *et al*. 2002; Pataki *et al*. 2002). In principle, a respiring source changes the ambient CO_2 mixing ratio and its isotopic composition. The isotopic composition of the respiring source can be deduced from the two end-member mixing relationship, on the assumption that a canopy is a well-mixed vessel (Keeling 1958). However, plant canopies are not well-mixed vessels. Drag and shear imposed on the atmosphere by plants causes the turbulent transfer of trace gases between plants and the atmosphere to be intermittent and to occur against the mean scalar concentration gradient (Raupach, Finnigan & Bruwet 1996; Finnigan 2000). Furthermore, vertical variations in leaf photosynthetic capacity and canopy structure cause respiratory carbon fluxes to vary vertically throughout the canopy. Another source of variation associated with the measurement of Keeling plot intercepts arises from logistical and technological issues that compromise sampling frequency and density. Air samples must be collected in flasks and returned to a laboratory for analysis on a mass spectrometer. This time-consuming and expensive procedure limits the number of samples that can be collected and analysed during a given period, thereby producing a sample mean with a less than ideal sampling error. Quantitatively, the relative sampling error of an atmospheric trace gas concentration profile is a function of the time scale of turbulence, τ, and the time duration over which the entire profile is measured, T_c (Meyers *et al*. 1996):

$$\varepsilon = 6\left(\frac{T_c}{\tau}\right)^{0.8} \quad (1)$$

From Eqn 1, we deduce that the relative sampling error equals 35% when the isotopic profile is sampled only once every 30 min and the turbulence time scale is 200 s. In contrast, a relative sampling error of less than 5% can be attained if the profile is sampled every minute; but this metric is not realistic when using a mass spectrometer at a distant laboratory. Implementing a less than ideal sampling frequency may be one source of variance associated with complex carbon isotope profiles reported in the literature (Medina & Minchin 1980; Schleser & Jayasekera 1985; Garten & Taylor 1992; Kruijt *et al*. 1996; Flanagan *et al*. 1996; Buchmann *et al*. 1997a; Buchmann, Kao & Ehleringer 1997b; Buchmann & Ehleringer 1998; LeRoux *et al*. 2001) and spatial variations of carbon dioxide sources and sinks may contribute to a controversy as to whether or not Keeling plot intercepts vary with time of day; the literature contains examples showing that the Keeling-plot intercepts for carbon isotopes do (Bowling, Baldocchi & Monson 1999a; Pataki *et al*. 2002) and do not change from night to day (Buchmann & Ehleringer 1998, Mortazavi & Chanton 2002).

In this article, we intend to evaluate carbon isotope measurements through the theoretical lens of a biometeorologist. Mechanistic biophysical models that couple micrometeorological and eco-physiological theories have the potential to shed light on how leaf-level relationships for isotopic discrimination can be integrated to the canopy and landscape dimensions. This capability exists because these models are able to resolve vertical profiles of carbon isotope discrimination with high vertical resolution and they can account for counter-gradient transfer (Katul & Albertson 1999; Lai *et al*. 2000; Baldocchi & Wilson 2001). Second, biophysical models can predict how isotope discrimination may respond to environmental perturbations. and third, biophysical models can produce information on the diurnal, seasonal and interannual dynamics of isotope discrimination. The value of this third feature stems from the fact that few long-term studies on isotope discrimination exist (e.g. Lowdon & Dyck 1974; Flanagan *et al*. 1996; Buchmann *et al*. 1997a, b; Damesin, Ramball & Joffre 1998; Bowling *et al*. 2002) due to the economic and logistical constraints of using mass spectrometers to analyse air samples.

Only a few biophysical models have been developed to assess stable carbon discrimination between a plant canopy and the atmosphere. To date, the majority of models have been developed for global scale applications (Lloyd & Farquhar 1994; Ciais *et al*. 1995; Fung *et al*. 1997). Of the models developed for studying carbon isotopic exchange in the surface boundary layer, two use 'big-leaf' theory (Lloyd *et al*. 1996; Bowling *et al*. 2001) and the others use Lagrangian localized near field (LNF) diffusion theory (Kruijt *et al*. 1996; Raupach 2001). 'Big leaf' models have self-acknowledged limitations. For example, they presuppose that a forest is physically and biochemically homogeneous, a false assumption in many circumstances as noted by reports of vertical gradients in isotopic discrimination (e.g. Garten & Taylor 1992; Buchmann & Ehleringer 1998). Lagrangian LNF theory has the potential to account for counter-gradient transfer. Yet, this modelling framework makes many simplifying assumptions about the heterogeneity of turbulence in the canopy (e.g. Warland & Thurtell 2000) and the quantification of sources and sinks. Furthermore, it ignores the effect of atmospheric stability on turbulent diffusion, which has an important impact on scalar fluxes and concentration fields inside canopies (Baldocchi & Harley 1995; Leuning 2000).

Biophysical models, such as *CANOAK* (Baldocchi & Harley 1995; Baldocchi 1997; Baldocchi & Wilson 2001), can be used to address many of the issues related to the interpretation of stable carbon isotopes in air and ecosystem components. First, *CANOAK* accounts for counter-gradient transfer and heterogeneous canopy turbulence

by using a Lagrangian random-flight turbulent transfer scheme. Second, its multilayer architecture enables it to assess sources and sinks and trace gas, mixing ratios with high vertical resolution. These attributes give the model the potential to interpret Keeling plots intercepts during the day and night. Third, by coupling leaf energy balance, photosynthesis and stomatal conductance, *CANOAK* is able to examine interrelationships between water use efficiency, isotope discrimination and vapour pressure deficits with mechanistic detail. Fourth, its integration of algorithms that assess photosynthesis, stomatal conductance and radiative transfer through the canopy gives it the potential to diagnose how variations in canopy structure and photosynthetic capacity may alter isotope discrimination. and finally, by incorporating information on how leaf area index and physiological capacity vary over the growing season, a biophysical model, like *CANOAK,* has the potential to investigate how a forest canopy discriminates against ^{13}C on daily, seasonal and yearly time scales.

In this paper, we describe adaptations that were made to the *CANOAK* model to enable it to simulate flux densities and concentration profiles of $^{13}CO_2$ within and above a deciduous forest. We then compare model computations and measurements of isotopic fluxes and discrimination made during experiments at Walker Branch in 1998 (Bowling *et al*. 1999a, 2001). Finally, we discuss model computations were that performed to examine:

1 vertical profiles and diurnal and seasonal patterns in whole-canopy carbon isotope discrimination (Δ_{canopy});
2 the impact of variation in environmental variables (light, humidity deficits) on Δ_{canopy}; and
3 inter-relationships between $\Delta_{canopy,}$ stand-level water use efficiency and humidity deficits.

MATERIALS AND METHODS

Model: theory, implementation, inputs and parameters

CANISOTOPE is a one-dimensional, multilayer biosphere–atmosphere gas exchange model that computes water vapour, CO_2 and sensible heat flux densities and the microclimate within and above a forest. The model, a member of the *CANVEG*/*CANOAK* family, consists of coupled micrometeorological and eco-physiological modules. The micrometeorological modules compute leaf and soil energy exchange, turbulent diffusion, scalar concentration profiles and radiative transfer through the canopy. Environmental variables, computed with the micrometeorological module, drive the physiological modules that compute leaf photosynthesis, stomatal conductance, transpiration and leaf, bole and soil/root respiration. The model has been described and tested for summer-length studies by Baldocchi & Harley (1995) and Baldocchi (1997) and over the course of several years by Baldocchi & Wilson (2001). A brief overview of key components is provided below.

The conservation budget for a passive scalar provides the foundation for computing scalar flux densities (F) and their mixing ratio (C). By assuming that the canopy is horizontally homogeneous and environmental conditions are steady, the scalar conservation equation becomes an equality between the change, with height, of the vertical turbulent flux density (F) and the diffusive source/sink strength, $S(C,z)$. For $^{13}CO_2$, the conservation budget is expressed as (after Raupach 2001):

$$\frac{d^{13}C}{dt} = \frac{d(R_a \cdot C)}{dt} = -\left(\frac{\partial (R_a \cdot F(C,z))}{\partial z}\right) + S(^{13}C, z) \quad (2)$$

where R_a equals the ratio $^{13}C/(^{12}C + ^{13}C)$. The source/sink term is a function of the diffusion of $^{13}CO_2$ across a network of laminar boundary layers, the rate by which $^{13}CO_2$ is assimilated by leaves and the rate it is respired by the vegetation and soil.

Photosynthesis of $^{13}CO_2$ (^{13}A) is defined as a function of leaf photosynthesis (A) and the ratio $^{13}C/(^{12}C + ^{13}C)$ in the photosynthetic products (R_{plant}); alternatively ^{13}A can be expressed in terms of R_a and Δ, the isotopic discrimination factor due to photosynthesis:

$$^{13}A = A \cdot R_{plant} = \frac{A \cdot R_a}{1 + \Delta} \quad (3)$$

Leaf photosynthesis is computed as a balance between the supply and demand for carbon dioxide. The supply is limited by the diffusion of carbon dioxide through the leaf boundary layer and stomata. Stomatal conductance (g_s) is computed with the algorithm of Collatz *et al*. (1991), which couples stomatal conductance with leaf photosynthesis, relative humidity and the CO_2 concentration at the leaf's surface (C_s). The biochemical demand for CO_2 by leaf photosynthesis (A) is constrained by the interaction between the intercellular CO_2 concentration, C_i, and the rates of carboxylation (V_c), oxygenation (V_o, photorespiration) and dark respiration (R_d) (Farquhar, von Caemmerer & Berry 1980).

The isotopic discrimination factor due to photosynthesis, Δ, is defined as:

$$\Delta = \left(\frac{R_a}{R_{plant}} - 1\right) \quad (4)$$

(Δ is commonly multiplied by 1000 and expressed in dimensionless units of per mil, ‰). We calculated the photosynthetic discrimination against $^{13}CO_2$ with a linear model that is a function of the CO_2 mixing ratio inside the substomatal cavity of the leaf (C_i), relative to its mixing ratio in the atmosphere, C_a (Farquhar O'Leary & Berry 1982):

$$\Delta = a + (b - a)\frac{C_i}{C_a} \quad (5)$$

In Eqn 5, a is the isotopic fractionation that occurs during diffusion (4·4‰) and b is the net fractionation due to carboxylation (27·5‰). This algorithm is a simpler version of the more expansive model produced later by Farquhar *et al*. (1989) that includes additional terms for fractionation across the laminar boundary layer, an equilibrium fractionation as CO_2 enters solution and a fractionation term representing $^{13}CO_2$ diffusion in water. The internal CO_2

concentration was computed using a conductance relationship between leaf photosynthesis and stomatal conductance, $C_i = C_s - (A/g_s)$ (Farquhar *et al*. 1980).

Respiration provides energy for metabolism and synthesis. At the leaf level, we assess dark respiration as a function of photosynthetic capacity (Collatz *et al*. 1991) and temperature. Soil and bole respiration is computed with a relation based on the temperature-dependent Arrhenius equation (Hanson *et al*. 1993). The isotopic signal of plant respiration is assumed to equal that produced by the previous day's photosynthesis; this assumption will be refined as more data become available (e.g. Bowling *et al*. 2002). Soil respiration of $^{13}CO_2$ is represented as a multiplicative function of soil respiration, F_{soil}., and the isotope ratio of total ecosystem respired CO_2, R_{soil}. In the model simulations we assigned R_{soil} the value derived from Keeling plot measurements, *in lieu* of any other information (Bowling *et al*. 1999a, 2002).

The transfer of photons through the canopy is simulated to evaluate the flux densities of visible, near infrared and long-wave radiation, the probability of sunlit and shaded leaves, as well as photosynthesis, stomatal conductance, and leaf and soil energy balances. The radiative transfer model is derived from Norman (1979) and considers the impact of clumped foliage on the probability of beam penetration using a Markov chain model (Baldocchi & Harley 1995).

The interdependence between sources and sinks $[S(C,z)]$ and scalar concentrations $[C(z)]$ requires the use of a turbulent diffusion model. A Lagrangian turbulence transfer scheme (Raupach 1988, 2001) is used to compute turbulent transport and diffusion. With regard to the Lagrangian model, concentration differences between an arbitrary level (C_z) and a reference level (C_r) (located above a plant canopy) are computed by summing the contributions of material diffusing to or from different layers in the canopy (Raupach 1988, 2001). A dispersion matrix is computed using a stochastic differential equation that tracks the diffusion of an ensemble of fluid parcels as they travel through a virtual atmosphere (Thomson 1987). The random flight algorithm accounts for heterogeneity of turbulence inside the canopy and the impact of atmospheric thermal stability on the variance of vertical velocity fluctuations (Baldocchi & Harley 1995).

Leaf boundary layer resistances for molecular compounds are computed using flat plate theory (Schuepp 1993) for free and forced convection. To simulate wind speed, we apply the logarithmic wind law above the canopy and the exponential wind profile within it.

Leaf temperature is calculated by solving the leaf energy balance (Norman 1979). This information is used to determine enzymatic rates associated with carboxylation, electron transport, and respiration and to evaluate transpiration, sensible heat fluxes and infrared emission.

Soil constitutes the lowest boundary of a canopy-scale, water vapour, CO_2 and trace gas exchange model. Flux densities of convective and conductive heat transfer and evaporation at the soil/litter boundary and soil temperature profiles are computed using a 10-layer numerical soil heat transfer model (Campbell 1985).

A suite of external meteorological variables is used to drive the model and provide the upper boundary conditions for the model calculations. These variables include shortwave radiation, air and soil temperature, relative humidity, wind speed, and CO_2 and $^{13}CO_2$ concentrations at a reference level above the canopy. Based on the local time, longitude and latitude, the model first computes the sun angle. Next the model computes photon transport through the foliage space, by dividing the canopy into 40 layers of equal leaf area. These computations produce estimates of flux densities of visible, near infrared and infrared radiation and the fractions of sunlit and shaded leaf area. Next, solar radiation information is used to produce an initial estimate of stomatal conductance. In turn, these products are used to compute leaf photosynthesis, leaf energy fluxes (latent and sensible heat), leaf temperature, and respiration. Information on scalar source/sink strengths (water vapour, heat, CO_2 and $^{13}CO_2$) and turbulent mixing are used to compute scalar profiles of temperature, humidity, CO_2 and $^{13}CO_2$ within and above the canopy. Iterations are performed on revised estimates of long wave radiation emission, stomatal conductance and scalar source–sink strengths for heat, water vapour, CO_2 and $^{13}CO_2$ until equilibrium is achieved between the flux profiles and their local scalar fields.

Two key plant input parameters in *CANISOTOPE* are leaf area index and the maximum carboxylation rate, V_{cmax}. Data on leaf photosynthetic properties were derived using gas exchange measurement on oak (*Quercus alba; Q. prinus*), maple (*Acer rubrum*) and black gum (*Nyssa sylvatica*) leaves (Harley & Baldocchi 1995; Wilson, Baldocchi & Hanson 2000). Values of photosynthetic model parameters used in the simulations are listed in Table 1. These rate coefficients are scaled according to leaf temperature (relative to an optimal temperature of 311 K), position within the canopy and time of year. Other biochemical rate constants, used for photosynthesis, such as the maximum rate of electron transport (J_{max}) and dark respiration rate (R_d) were scaled to the maximum carboxylation rate (V_{cmax}) (Wilson *et al*. 2000). We varied V_{cmax} with depth in the canopy to reflect its dependency on vertical variations in spe-

Table 1. Parameter values used by the *CANISOTOPE* model in the simulations of canopy CO_2, water vapour and energy exchange during the peak summer growing season

Parameter	Value	Units
V_{cmax} (311 K)	73	μmol m^{-2} s^{-1}
J_{max} (311 K)	2·32 V_{cmax} (311 K)	μmol m^{-2} s^{-1}
R_d	0·0046 V_{cmax} (311 K)	μmol m^{-2} s^{-1}
LAI max	6	m^2 m^{-2}
Canopy height	26	m
Leaf length	0·10	m
Stomatal conductance factor	9·5	–
Quantum yield	0·055	mol mol^{-1}
Markov clumping factor	0·84	–

cific leaf weight and leaf nitrogen content. Seasonal variations in V_{cmax} were linked to seasonal changes in leaf area index. The seasonal change in photosynthetic capacity was computed to vary as a fraction of full leaf area, which is a simpler representation of the results reported by Wilson *et al*. (2000). The suite of micrometeorological measurements used to drive and test model computations are described in Baldocchi & Wilson (2001).

Site characteristics

The Walker Branch Watershed experimental field site is located on the United States Department of Energy reservation near Oak Ridge, Tennessee (lat. 35°57′30″ N; long. 84°17′15″ W; 335 m above mean sea level). The mean annual rainfall is 1372 mm and the mean annual air temperature is 13·9 °C.

The site is classified as an Eastern, mixed-species, broadleaved deciduous forest. The predominant species in the forest stand are oak (*Quercus alba* L., *Quercus prinus* L.) and maple (*Acer rubrum* L., *Acer saccharum*). The forest has been growing since agricultural abandonment in 1940. The mean canopy height is about 26 m. The peak leaf area index is about 6·0 and generally occurs by day 140.

Measurements, instrumentation and flux density calculations

Air samples were collected in whole-air flasks at six heights (0·75, 2, 4, 10, 26 and 44 m) for analyses of CO_2 and isotope mixing ratios. Details of this system are reported in Bowling *et al*. (1999a). Flask samples were collected during periods between 14 (day 195) and 17 (day 198) July 1998, at the canopy top (26 m). On 15 July (day 196), three flasks were filled at 0·75, 26 and 44 m. Samples were also collected at night at a variety of heights on 13 and 14 July.

It is common practice to express the isotopic mole fraction as a ratio of the isotope content of a sample and a known standard because the absolute isotope content is difficult to measure: $\delta^{13}C = \left[\frac{^{13}C/C|_{\text{sample}}}{^{13}C/C|_{\text{standard}}} - 1\right] \times 1000$; the units of $\delta^{13}C$ are per mil, ‰. The isotopic standard is derived from a carbonate formation in South Carolina, called Pee Dee Belemnite and is expressed in terms of total carbon, $^{13}C/(^{12}C + ^{13}C)$, as recommended by Tans, Berry & Keeling (1993).

The carbon isotope ratio in CO_2 were evaluated at the Stable Isotope Laboratory of the University of Colorado's Institute of Arctic and Alpine Research (INSTAAR) and CO_2 mole fractions were measured at National Oceanic and Atmospheric Administration (NOAA) Climate Monitoring and Diagnostic Laboratory (NOAA/CMDL), as described by Trolier *et al*. (1996). The precision for our flask measurements was 0·1 p.p.m. for CO_2 and 0·03‰ for $\delta^{13}C$.

The eddy covariance method was used to measure CO_2, water vapour and sensible heat flux densities. These measurements were made using a three-dimensional sonic anemometer and an open-path, infrared absorption gas analyser (Auble & Meyers 1992). The instruments were suspended at 36 m, about 10 m above the forest.

Flux densities of carbon isotopes, and their derived quantities, were measured using two inferential methods. The first method (referred to as the eddy covariance (EC)/flask method) is based on the linear relation between isotopic composition ($\delta^{13}C$) and CO_2 mixing ratio, C. We then combined this information with high frequency measurements of CO_2 mixing ratio to compute high frequency variations in $\delta^{13}C$. Finally, we calculated the isotopic flux density, $F_{\delta^{13}C}$, known as the isoflux (Bowling *et al*. 1999a, 2001) as:

$$F_{\delta^{13}C} = \rho_a \overline{w'\left[(\delta^{13}C)\cdot C\right]'} \approx \rho_a \overline{w'[(mC+b)\cdot C]'} \quad (6)$$

In Eqn 6, the overbar denotes time averaging (30 min), the primes denote fluctuations from the mean, m is the slope of the linear regression between $\delta^{13}C$ and C and b is its intercept. For clarification, we also note that Eqn 6 is a linear combination of the flux density of ^{13}C, $F_{^{13}C} = \rho_a \overline{w'^{13}C'}$.

Equation 6 is derived from the steady-state version of conservation budget for the iso-concentration, $\delta^{13}C \cdot C$ (Raupach 2001):

$$\frac{d(\delta^{13}C)\cdot C}{dt} = -\left(\frac{\partial(\delta^{13}C)\cdot F(z)}{\partial z} + \delta_s \cdot S(^{13}C, z)\right) \quad (7)$$

Undefined terms in Eqn 7 are S, the source-sink strength, and δ_s the isotopic composition of the source (plant or soil) or sink (plant) material. As Eqn 7 is expressed in terms of delta-notation, fluxes towards the canopy are positive when there is a loss of $^{13}CO_2$ from the atmosphere; contrary, fluxes are negative when directed towards the canopy when one considers the budget equation for scalar, ^{13}C.

The second isotopic flux measurement method used the hyperbolic relaxed eddy accumulation (HREA) technique (Bowling *et al*. 1999a,b). This technique collects air in updraughts and downdraughts. Isotopic flux densities are proportional to the standard deviation of the vertical velocity (σ_w) and the iso-concentration differences between the air captured in the up and down draught samplers, $F_{\delta^{13}C} \sim \sigma_w\left[(\delta^{13}C\cdot C)|_{up} - (\delta^{13}C\cdot C)|_{down}\right]$.

RESULTS AND DISCUSSION

Model validation

Our first intention was to show how well the *CANISOTOPE* model could reproduce measured concentrations of the stable carbon isotope, $^{13}CO_2$, by testing our ability to reproduce Keeling plot intercepts, as deduced from comparisons between vertical profiles of $\delta^{13}C$ and CO_2 (Fig. 1). During the nocturnal period of day 194 the Keeling plot intercept deduced from gas measurements was –26·13 ± 0·56‰; we used the geometric mean regression method to estimate regression intercepts. By comparison, the Keeling plot intercept produced by the model was –26·26 ± 0·01‰, a difference of 0·13‰ or less than 1%. We thereby conclude that there is no statistical difference

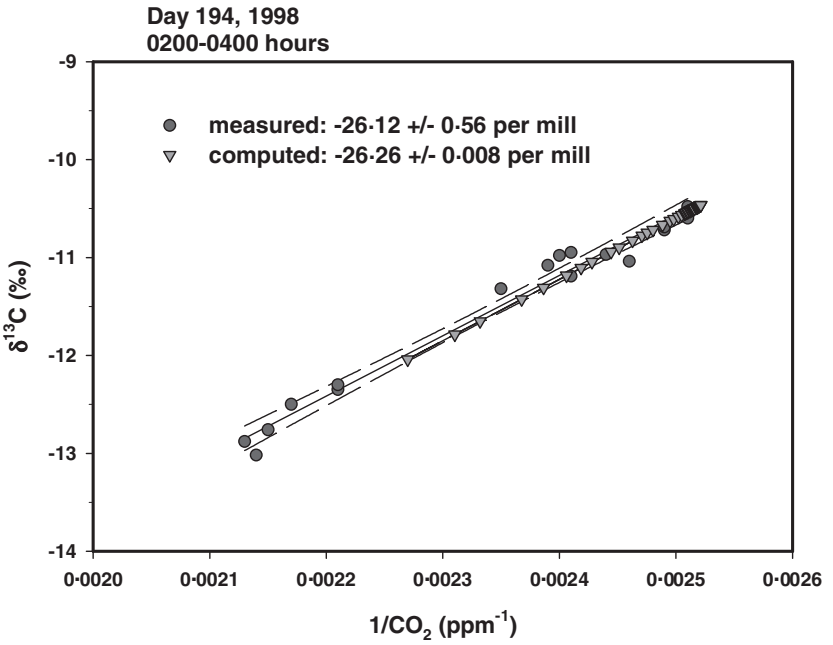

Figure 1. Computed and measured Keeling plots during the night-time period of day 194, 1998. The intercepts of the Keeling plots were determined using the geometric mean regression method. The Keeling intercept from the field measurements is –26·12 ± 0·56‰. The intercept deduced from model computations is –26·26 ± 0·01‰. The solid line is the linear regression and the dashed line represents the 95% confidence interval.

between the measured and computed Keeling plot intercept within the 95% confidence interval, using Students' *t*-test.

This favourable agreement may have been expected a *priori* because we used the measured Keeling plot intercept as the boundary condition for soil respiration in the model computations. However, this result is non-trivial because there was no guarantee that the model computations would converge with the measurements because counter-gradient transfer can occur throughout the canopy and because we computed the isotopic signal of the respiring foliage independently from the soil.

The second means of testing the model involves a comparison between measured and computed values of carbon isotope discrimination, Δ. Isotopic contents of leaves sampled through the canopy are presented in Table 2 and these data are plotted against model computations in Fig. 2.

The computed mean vertical profile of isotope discrimination, Δ, matched measured values of Δ within the sampling error of the model computations at most levels in the canopy; the computed values are based on the average photosynthesis on day 194, between 0800 and 1800 h. Factors relating to representativeness account for some of the differences observed. For example, the measured values reflect the isotopic signal the leaves had acquired during their lifespan of approximately 90 d, whereas the computations are representative of a single summer day.

As the number of leaves sampled was limited, we refer the reader to data from a prior and independent experiment near this field site for an additional source of model comparison data. Between 1984 and 1989, Garten & Taylor (1992) sampled and measured $\delta^{13}C$ values on leaves of trees growing on the Walker Branch Watershed. They reported that $\delta^{13}C$ for a cohort of maple (*Acer rubrum*), oak (*Quercus* spp.) and tulip poplar (*Liriodendron tulipifera*) leaves ranged between –28·8‰ and –30·1‰. We transformed $\delta^{13}C$ to Δ [$\Delta = (\delta_a - \delta_p)/(1 + \delta_p)$]) by assuming the isotopic value of the air (δ_a) during the mid 1980s was –7·7‰ (Francey *et al*. 1995). This assumption produced estimates of Δ that ranged between 20·5‰ and 21·8‰, which are consistent with our calculated values (Table 2; Fig. 2).

How we treat the isotopic signal of respiring leaves may contribute to the small biases between measured and computed discrimination values. At present we have two options. We can either set the signal of the leaves to that respired by the soil or have it reflect the isotopic signature of assimilated carbon. At present we are setting the isotopic ratio of carbon respired by leaves on the basis of the isotopic signal determined from the previous day's photosynthetic discrimination. Turnover times of respired carbon due to disequilibrium effects will influence how accurate the two assumptions are. If the turnover time for an appreciable fraction of respired CO_2 is several days to weeks, as recently reported by Högberg *et al*. 2001) and Bowling *et al*. (2002), then a third option will be needed, which is based on a short-term carbon accounting.

Table 2. Carbon isotope composition of leaves, $\delta^{13}C$ (from Bowling *et al*. 1999a). Carbon isotope discrimination was computed assuming $\delta^{13}C$ of air was –8·00‰

Species	Position in canopy	$\delta^{13}C$ (‰)	Δ(‰)
Quercus alba	Top (26 m)	–28·8	21·4
	Mid (20 m)	–30·0	22·7
	Bottom (10 m)	–30·1	22·8
Acer rubrum	Top (26 m)	–28·2	20·8
	Mid (20 m)	–29·6	22·3
	Bottom (10 m)	–30·2	22·9
Quercus prinus	Top (26 m)	–28·9	21·5
Liriodendron tulipifera	Top (26 m)	–28·4	20·7

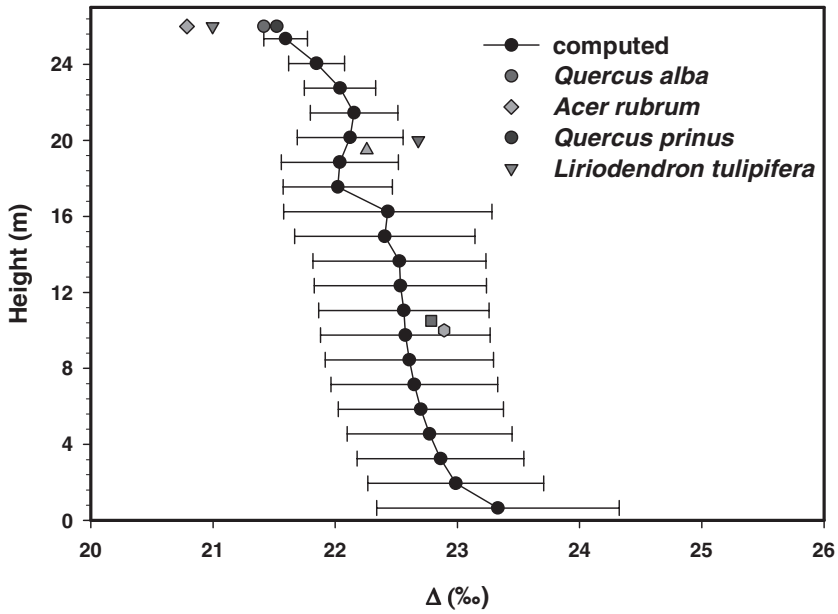

Figure 2. Vertical profiles of carbon isotope discrimination, both computed and measured, for a summer day (D194) between 0800 and 1800 h. Error bars denote the modelled sampling error and were determined from standard error of the mean over the course of the day.

The third means of testing the model involves a comparison between computed and measured isofluxes. Figure 3 shows that the model reproduced the magnitude and diurnal pattern observed with the HREA method with reasonable fidelity, considering potential errors in the isoflux measurement, as well as the model. On average isofluxes ranged between 30 and 600 μmol m^{-2} s^{-1}‰ over the course of three summer days and peaked around midday.

Figure 4 shows a second test of the ability of the model to compute isofluxes, but against measurements produced with the eddy covariance/flask sampling method (Eqn 6). This test has a larger sample size, but the measurements also exhibit more run-to-run variability. Model computations tended to overestimate inferred measurements around midday and a phase shift between model computations and measurements occurred in the morning, with calculations leading measurements.

To provide a quantitative comparison between measurements and calculations, we fitted the measured and computed diurnal patterns of isotopic flux densities with second-order polynomials and integrated the regressions to compute daytime mean flux densities. Between 0700 and 1800 h, the daytime integrals of isotopic fluxes were 529, 404 and 369 μmol m^{-2} s^{-1}‰ for the model calculations, the HREA and EC/Flask measurements, respectively. As both the measurement technology and the model scheme are in

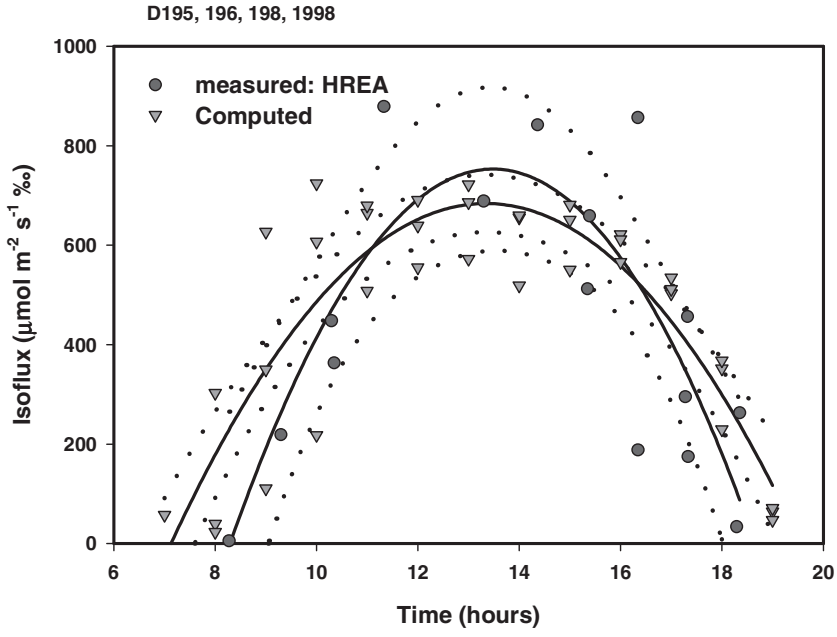

Figure 3. A comparison between measured and computed values of the ^{13}C isotopic flux for three summer days (D195, 196, 198) in 1998. The field data are reported in Bowling *et al*. (1999a) and were evaluated using the hyperbolic relaxed eddy accumulation technique (HREA). The solid lines represent nonlinear regression fits. The dashed lines represent the 95% confidence interval.

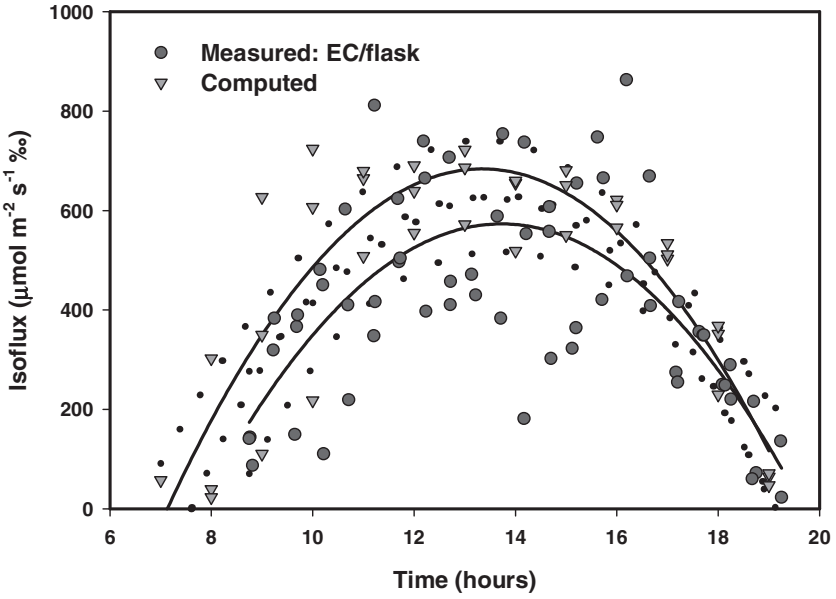

Figure 4. A comparison between measured and computed values of the ^{13}C isotopic flux for three summer days (D195, 196, 198) in 1998. The field data are reported in Bowling *et al*. (1999a) and were evaluated using the modified eddy covariance/flask method (EC/flask). Black dotted lines are the 95% confidence interval. The solid line is the regression fit.

the development stages it is too premature to indict one method or the other. We can only claim that the model reproduces the diurnal pattern and that the magnitude of modelled and measured isotopic flux densities agree with one another within 30%.

Diurnal and seasonal trends in isotope discrimination

No long-term and continuous measurements of isotope discrimination by leaves exist in the literature. To provide insight on how these variables may change over the course of a growing season and respond to environmental perturbations we present computations derived from the *CANISOTOPE* model.

First we examine the diurnal variability of the canopy scale carbon isotope discrimination, Δ_{canopy}. Canopy scale values of carbon isotope discrimination (Δ_{canopy}) are computed by weighting leaf-scale values by photosynthesis and integrating with respect to height (Lloyd *et al*. 1996):

$$\Delta_{canopy} = \frac{\int_0^h \Delta(z)A(z)\mathrm{d}z}{\int_0^h A(z)\mathrm{d}z} \quad (8)$$

The variation of the mean canopy value of Δ_{canopy} over the course of the growing season is shown in Fig. 5. The most notable observation is how the diurnal range of Δ_{canopy} varies over the course of the growing season. The diurnal

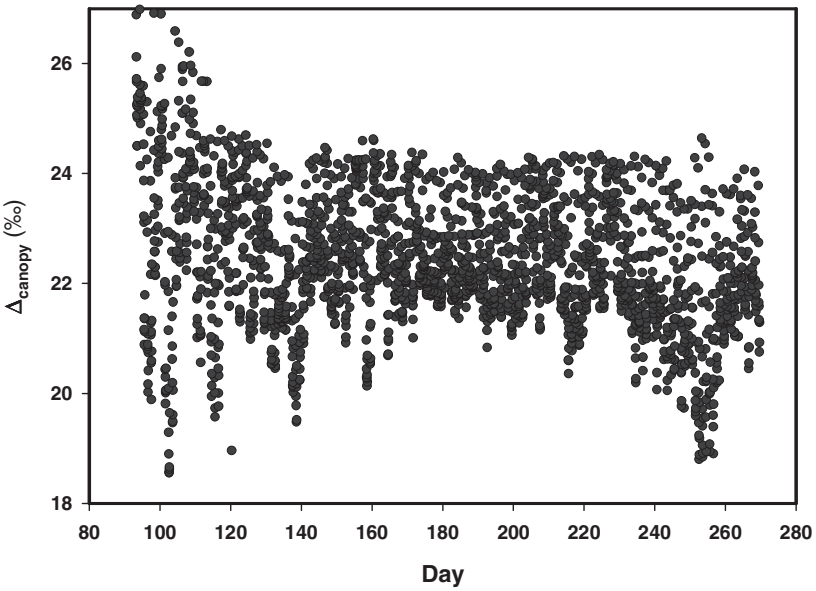

Figure 5. Seasonal change in hourly values of ^{13}C isotope discrimination computed during daylight periods.

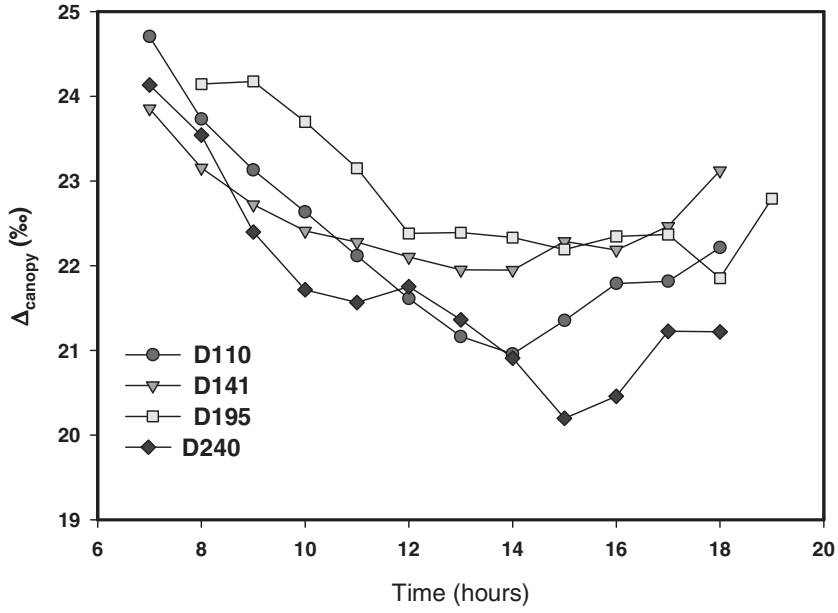

Figure 6. Computations of the diurnal pattern of carbon discrimination for four days during the 1998 growing season.

amplitude is greatest in the spring and autumn when discrimination values as low as 18‰ are computed. During the middle of the growing season (days 150 and 230), the Δ_{canopy} varies between 21·5 and 24·5‰, a range of 3‰. Over the course of the growing season, the mean value of Δ_{canopy} is 22·4‰.

In Fig. 6 we examine the diurnal pattern of Δ_{canopy} for four case days, distributed across the 1998 growing season. Day 110, a cool (15 °C) and sunny day, is representative of the spring leaf expansion phase when leaf area and photosynthetic capacity were low. The second case, day 141, was a warm (29 °C) and sunny day after the canopy attained full leaf. Case three, day 195, was a mild (25 °C) and partly cloudy summer day, during the field experiment. and case four, day 240, was a hot (32 °C), clear day near the end of the summer growing season. For all cases, greatest Δ_{canopy} values occur near sunrise and sunset, when photosynthesis rates diminish relative to respiration, the stomata close and C_i/C_a approaches one. Minimum Δ_{canopy} values typically occur during mid-afternoon (1400–1500 h). This is when the day's highest vapour pressure deficits occur because air temperatures are warmest and dry air is entraining from above the planetary boundary layer. These factors combine to lower stomatal conductance, independent of changes in photosynthesis, and thereby force C_i/C_a and Δ_{canopy} to be lower. With regard to seasonal changes in the diurnal pattern, the greatest amplitude and the lowest mid-afternoon values occur for the cases early in the spring (D110) and hot, late summer (D240).

Response to the environmental and plant functional variables

Diurnal and seasonal variations in light, humidity, and temperature impose corresponding changes in photosynthesis, transpiration and stomatal conductance. In this section we investigate the sensitivity of isotope discrimination to several external environmental forcings.

Figure 7 shows the light response curve for Δ_{canopy} over the course of the growing season. Consistent with the diurnal pattern shown in Fig. 6, we observe the greatest values of Δ_{canopy} when photosynthetic photon flux density, Q_p, is low and lower discrimination when Q_p is maximal. The second feature of note is that the canopy-scale, light response curve for carbon isotope discrimination is quasi-linear. This observation is consistent with light response curves for photosynthesis of forest canopies (Baldocchi & Harley 1995; Baldocchi 1997).

Noted in Fig. 7 is a large amount of scatter. One source of variation is attributed to canopy photosynthesis being greater under cloudy skies than under clear skies given a similar value of Q_p (Baldocchi 1997). This situation would favour greater discrimination against $^{13}CO_2$ under cloudy conditions and an increase in Δ_{canopy}. A second source of variation involves interactions among the degree of cloudiness, vapour pressure deficit (D), C_i/C_a and Δ_{canopy}. The explanation follows. First, D is lower under cloudy skies than under clear skies (Gu *et al*. 2002). Secondly, the ratio C_i/C_a decreases as the atmosphere becomes drier (Fig. 8). In this circumstance, stomata close independent of their link to photosynthesis in dry air (Schulze 1986; Lloyd & Farquhar 1994). This physiological response forces C_i to be drawn-down inside the stomatal cavity until a new equilibrium between CO_2 supply and photosynthetic demand is met. A consequence of these interactions is a reduction in discrimination (Eqn 5).

Water use efficiency

The amount of carbon gained by photosynthetic assimilation (A) per unit water lost to transpiration (T) is referred to as the *instantaneous* water use efficiency (Farquhar &

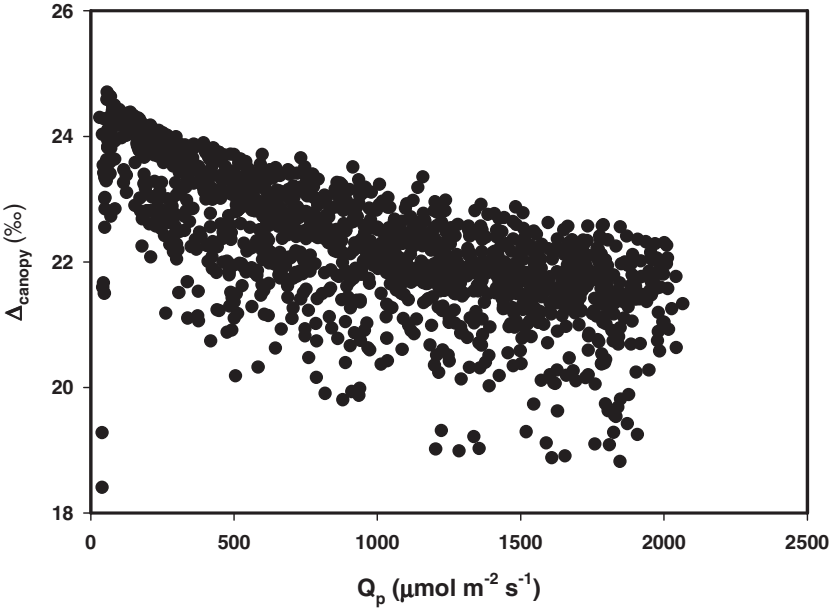

Figure 7. Response of ^{13}C discrimination to photosynthetic photon flux density when the canopy had achieved full-leaf, days 140–260, 1998.

Richards 1984; Condon *et al*. 1993) and is a function of the internal (C_i) and atmospheric (C_a) CO_2 concentrations and vapour pressure deficit, D, between a leaf and the atmosphere.

$$\frac{A}{T} = \frac{C_a\left(1 - \frac{C_i}{C_a}\right)}{1{\cdot}6 \cdot D} \tag{9}$$

Because internal CO_2 partial pressure, C_i, is positively correlated with the $^{13}CO_2$ discrimination, stable carbon isotopes have been used to evaluate water use efficiency, the ratio between photosynthesis (A) and transpiration (T) (Farquhar & Richards 1984; Farquhar *et al*. 1988, 1989; Condon *et al*. 1993). Conceptually, one expects instantaneous water use efficiency to increase as C_i/C_a, and by inference carbon isotope discrimination, decreases (Farquhar & Richards 1984; Farquhar *et al*. 1988). For this condition to hold, however, vapour pressure deficit must remain constant and be independent of Δ (Condon *et al*. 1993), an assumption that may not be true at the canopy scale.

Based on model computations presented in Fig. 9, there are interactions the field environment among stomatal conductance, C_i/C_a, vapour pressure deficits, and leaf temperature that result in A/T increasing with increasing isotopic discrimination. For example, model calculations indicate that a fivefold change in A/T can occur as Δ_{canopy} ranges between 20 and 23‰. The positive slope of the relation between instantaneous A/T and Δ_{canopy} is opposite to the observations derived from leaf biomass and water use stud-

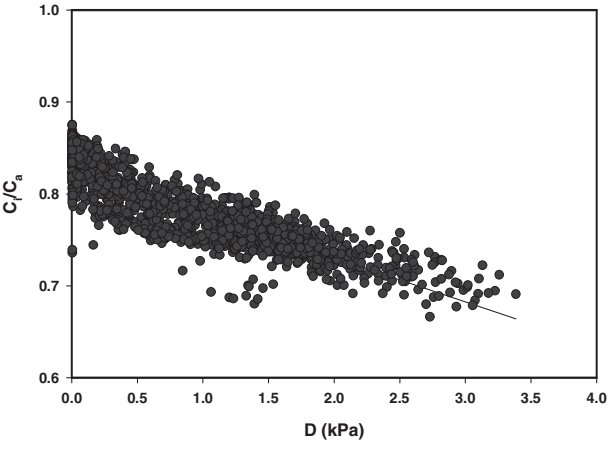

Figure 8. The impact of vapour pressure deficit (D) on computations of C_i/C_a, which are integrated throughout the canopy. The regression between the dependent and independent variables is linear with a coefficient of determination (r^2) equal to 0·75. The regression intercept and slope are 0·826 and –0·0481, respectively.

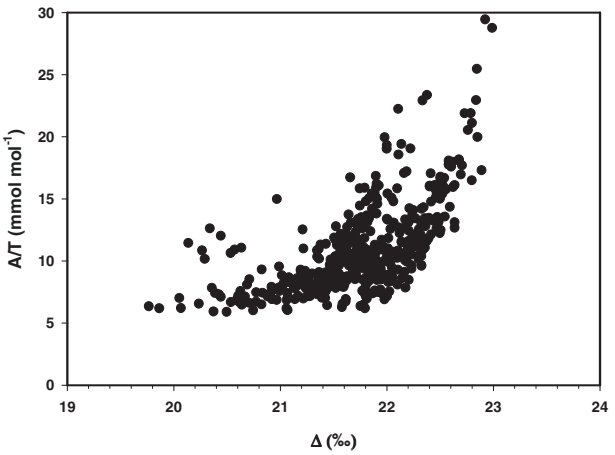

Figure 9. Computations of the relation between A/T and Δ_{canopy} during the 1998 growing season. This relation represents data on an hourly time scale.

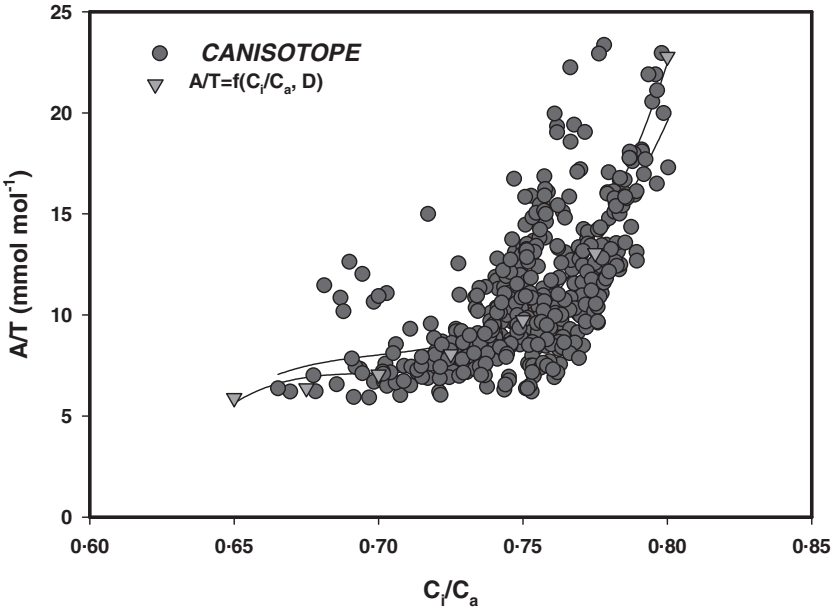

Figure 10. The relationship between water use efficiency and the ratio of internal to atmospheric CO_2 concentration during the 1998 growing season. The circles dots reflect computations based on field measurements over a temperate deciduous forest in Tennessee. The inverted triangles dots represent computations with the big-leaf model.

ies that are conducted on seasonal time scales. Condon *et al*. (1993) and Hall *et al*. (1993), for example, report that Δ is negatively correlated with D and A/T was positively correlated with D, although not significantly, for their study over dryland wheat. Farquhar & Richards (1984) show that A/T increases as $\delta^{13}C$ becomes less negative for wheat biomass studies. On the other hand, data presented in Fig. 9 are consistent with data from micrometeorological field measurements; typically, the ratio of carbon uptake to water loss, an index of water use efficiency, is negatively correlated with D (Baldocchi & Harley 1995; Arneth *et al*. 1998).

The *CANISOTOPE* model gives us the potential to provide a mechanistic and physiological explanation for these contradictory results. First one can demonstrate theoretically how water use efficiency at the stand scale relates to changes in C_i/C_a and carbon isotope discrimination by combining the negative relationship between Δ_{canopy} and D, produced in Fig. 8, with Eqn 9:

$$\frac{A}{T} = \frac{C_a\left(1-\frac{C_i}{C_a}\right)}{28{\cdot}32 - 33.2\frac{C_i}{C_a}} \qquad (10)$$

How well Eqn 10 captures the interactions between A/T, C_i/C_a and D is shown in Fig. 10. Here we compare estimates of A/T using the 'big-leaf'model (Eqn 10) against estimates derived from the *CANISOTOPE* model, which has a full accounting for leaf energy balance, vapour pressure deficit and stomatal conductance interactions. The two water use efficiency models produce calculations that overlap and predict that instantaneous water use efficiency increases with C_i/C_a, and by extension with increasing Δ_{canopy}, in a nonlinear manner. Water use efficiency increases most sensitively to increasing C_i/C_a, after it exceeds a threshold of about 0·75. Differing sensitivities of the numerator and denominator, in Eqn 10, to changes in C_i/C_a illustrate why canopy-scale A/T increases with increasing C_i/C_a, rather than decreases (Fig. 11).

Although these model computations may seem counterintuitive from a static view of how water use efficiency of leaves respond to changes in C_i/C_a, they are consistent with theory that consider the marginal cost of water (E) for carbon gain (A), $[(\partial E/\partial g)/(\partial A/\partial g)]$, at the leaf-scale (Cowan & Farquhar 1977; Thomas, Eamus & Bell 1999); this theory considers the effects of simultaneous changes in vapour pressure deficits and internal CO_2 on photosynthesis and transpiration as stomatal open and close. Furthermore, our computations of water use efficiency (which consider these feedbacks, but numerically) have been verified at the stand-scale in a previous paper using eddy covariance flux measurements across a range of humidity deficits (Baldocchi & Harley 1995).

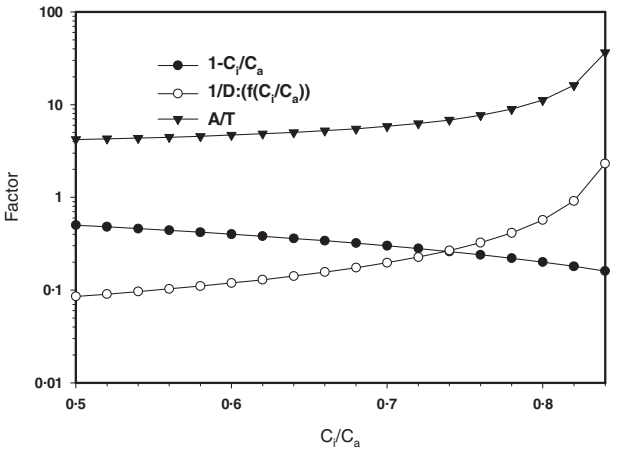

Figure 11. Decomposition of how the numerator and denominator of the function, A/T, responds to changes in C_i/C_a.

CONCLUSIONS

The biophysical model, *CANOAK*, was modified to compute fluxes and concentrations of the stable isotope of $^{13}CO_2$ over and within a deciduous forest. With recognition that carbon isotope flux measurement technology is in a nascent stage, we find that the agreement between measured and computed isofluxes was favourable, within 30%. Furthermore, the model was able to reproduce other metrics, such as the Keeling plot intercept and leaf discrimination values of leaves, Δ.

With a tested model in hand, we were able to explore the dynamics of isotopic carbon discrimination over the course of days and the growing season. The model allowed us to explore and hypothesize how values of Δ_{canopy} may respond to changes in light and humidity deficits and how Δ_{canopy} relates to changes in instantaneous water use efficiency. Through the lens of the model we were able to detect that short-term water use efficiency increased with increasing C_i/C_a and Δ_{canopy}, rather than decrease, as simple leaf models predict.

Factors contributing to the satisfactory performance of the *CANISOTOPE* model include its multilayer framework, its dependence on coupled and constraining processes, such as leaf energy exchange, turbulent transfer, photosynthesis and stomatal conductance, and its representation of these fluxes on separate sunlit and shaded leaf classes. This approach contrasts with that of simpler 'big-leaf models' (e.g. Lloyd *et al*. 1996; Bowling *et al*. 2001) that do not evaluate non-linear functions on sunlit and shaded fractions of the canopy and ignore feedbacks among leaf temperature, humidity and carbon, water and energy fluxes. Consequently, simpler 'big-leaf' models often perform less well, when their computations are compared against eddy flux measurements (Norman 1993; De Pury & Farquhar 1997; Baldocchi & Wilson 2001). Acknowledging that 'big-leaf' models are often preferred for practical applications, we were able to use the mechanistic *CANIOSOPE* model to produce and parameterize a 'big-leaf' water use efficiency model that is able to consider interactions between C_i/C_a and D.

Regarding future model development and tests, several issues emerge. This physiologically based model does not compute growth respiration explicitly. Incorporating algorithms that consider changes in root and bole growth and partition soil respiration according to root and microbial respiration will lead to improvements in the specification and dynamics of the isotopic signal of the soil. Unresolved modelling issues, that must be deferred until more data are available, include how to represent lags in the respired isotopic signature due to changes in photosynthesis resulting from stress induced by high vapour pressure and soil moisture deficits (Bowling *et al*. 2002).

We close by stating that it was our objective to produce model runs that could serve as a template for the generation of hypotheses that could be addressed in future field studies as new technologies emerge for making long-term carbon isotope flux measurements. At present, with the operation of many long-term eddy flux experiments our community has the potential to implement the EC/Flask method (Bowling *et al*. 1999a, 2001) on seasonal time scales. Within the next year or two we anticipate development of tunable diode lasers that can detect fluctuations of $^{13}CO_2$ with adequate resolution and accuracy and be operational on longer time scales (Baer *et al*. 2002).

ACKNOWLEDGMENTS

We thank Rolf Siegwolf for kindly providing the leaf isotopic analyses in Table 2 and Chris Still for providing an internal review for us. We are also grateful to Tom Conway at NOAA/CMDL and Jim White, Candice Urban-Evans, and Kim Elkins (CU/INSTAAR) who analysed the air samples.

D.R.B. was supported during this time by grants from NSF (ATM-9905717) and USDA (99-35101-772) to J. R. Ehleringer (University of Utah) and R. K. Monson (University of Colorado). D.D.B. is supported by the California Agricultural Experiment Station, by the US Department of Energy's Terrestrial Carbon Project and NASA's EOS Validation Program.

Any opinions, findings, and conclusions or recommendations expressed in this publication are those of the authors and to not necessarily reflect the views of NSF.

REFERENCES

Arneth A., Kelliher F.M., McSeveny T.M. & Byers J.N. (1998) Fluxes of carbon and water in a *Pinus radiata* forest subject to soil water deficit. *Australian Journal of Plant Physiology* **25,** 557–570.

Auble D.L. & Meyers T.P. (1992) An open path, fast response infrared absorption gas analyzer for H_2O and CO_2. *Boundary Layer Meteorology* **59,** 243–256.

Baer D.S., Gupta M., O'Keefe A. & Paul J. (2002) Off-axis integrated cavity output spectroscopy for trace gas detection. *Applied Physics (Lasers and Optics), (Vol. B)* in press.

Baldocchi D.D. (1997) Measuring and modelling carbon dioxide and water vapour exchange over a temperate broad-leaved forest during the 1995 summer drought. *Plant, Cell and Environment* **20,** 1108–1122.

Baldocchi D.D. & Harley P.C. (1995) Scaling carbon dioxide and water vapour exchange from leaf to canopy in a deciduous forest: model testing and application. *Plant, Cell and Environment* **18,** 1157–1173.

Baldocchi D.D. & Wilson K.B. (2001) Modeling CO_2 and water vapor exchange of a temperate broadleaved forest across hourly to decadal time scales. *Ecological Modeling* **142,** 155–184.

Bowling D.R., Baldocchi D.D. & Monson R.K. (1999a) Dynamics of isotope exchange of carbon dioxide in a Tennessee deciduous forest. *Global Biogeochemical Cycles* **13,** 903–921.

Bowling D.R., Delany A.C., Turnipseed A.A., Baldocchi D.D. & Monson R.K. (1999b) Modification of the relaxed eddy accumulation technique to maximize measured scalar mixing ratio differences in updrafts and downdrafts. *Journal of Geophysical Research* **104,** 9121–9133.

Bowling D.R., McDowell N., Bond B., Law B. & Ehleringer J. (2002) ^{13}C content of ecosystem respiration is linked to precipitation and vapor pressure deficit. *Oecologia* **131,** 113–124.

Bowling D.R., Monson R. & Tans P.P. (2001) Partitioning net

ecosystem carbon exchange with isotopic fluxes of CO_2. *Global Change Biology* **7,** 127–145.

Buchmann N. & Ehleringer J.R. (1998) CO_2 concentration profiles and carbon and oxygen isotopes in C_3 and C_4 crop canopies. *Agricultural and Forest Meteorology* **89,** 45–58.

Buchmann N., Guehl J.-M., Barigah T.S. & Ehleringer J.R. (1997a) Interseasonal comparison of CO_2 concentrations, isotopic composition, and carbon dynamics in an Amazonian Rainforest (French Guiana), *Oecologica* **110,** 120–131.

Buchmann N., Kao W.Y. & Ehleringer J.R. (1997b) Influence of stand structure on carbon-13 of vegetation, soils and canopy air within deciduous and evergreen forests in Utah, United States. *Oecologia* **110,** 109–119.

Campbell G.S. (1985) *Soil Physics with BASIC.* Elsevier Scientific Publishing, Amsterdam, The Netherlands.

Ciais P., Tans P.P., White J.W.C., Trolier M., Francey R.J., Berry J.A., Randall D.R., Sellers P.J., Collatz J.G. & Schimel D.S. (1995) Partitioning of ocean and land uptake of CO_2 as inferred by $\delta^{13}C$ measurements from the NOAA Climate Monitoring and Diagnostics Laboratory Global Air Sampling Network. *Journal of Geophysical Research* **100,** 5051–5070.

Collatz G.J., Ball J.T., Grivet C. & Berry J.A. (1991) Regulation of stomatal conductance and transpiration: a physiological model of canopy processes. *Agricultural and Forest Meteorology* **54,** 107–136.

Condon A.G., Richards R., A. Farquhar G. & D. (1993) Relationships between carbon isotope discrimination for water use efficiency and transpiration efficiency for dryland wheat. *Australian Journal of Agricultural Research* **44,** 1693–1711.

Cowan I.R. & Farquhar G.D. (1977) Stomatal function in relation to leaf metabolism and environment. *Symposium of the Society of for Experimental Biology* **31,** 471–505.

Damesin C. Ramball S. & Joffre R. (1998) Seasonal and annual changes in leaf $\delta^{13}C$ in two co occurring Mediterranean oaks: relations to leaf growth and drought progression. *Functional Ecology* **12,** 778–785.

De Pury D. & Farquhar G.D. (1997) Simple scaling of photosynthesis from leaves to canopies without the errors of big-leaf models. *Plant, Cell and Environment* **20,** 537–557.

Ehleringer J.R. Buchmann N. & Flanagan L.B. (2000) Carbon isotope ratios in belowground carbon cycle processes. *Ecological Applications* **10,** 412–422.

Ehleringer J.R. Cerling T.E. & Helliker B.R. (1997) C_4 photosynthesis, atmospheric CO_2 and climate. *Oecologia* **112,** 285–299.

Ehleringer J.R. Hall A.E. & Farquhar G.D. (eds) (1993) *Stable Isotopes and Plant Carbon–Water Relations*. Academic Press, San Diego, CA, USA.

Farquhar G.D. & Richards R.A. (1984) Isotopic composition of plant carbon correlates with water use efficiency of wheat genotypes. *Australian Journal of Plant Physiology* **11,** 539–552.

Farquhar G.D. von Caemmerer S. & Berry J.A. (1980) A biochemical model of photosynthetic CO_2 assimilation in leaves of C_3 species. *Planta* **149,** 78–90.

Farquhar G.D. Ehleringer J.R. & Hubick K.T. (1989) Carbon isotope discrimination and photosynthesis. *Annual Review of Plant Physiology and Plant Molecular Biology* **40,** 503–537.

Farquhar G.D. Hubrick K.T. Condon A.G. & Richards R.A. (1988) Carbon isotope fractionation and plant water use efficiency. In *Stable Isotopes in Ecological Research* (eds P. Rundel, J.R. Ehleringer & K.A. Nagy), pp. 21–40. Springer Verlag, New York, USA.

Farquhar G.D. O'Leary M.H. & Berry J.A. (1982) On the relationship between carbon isotope discrimination and the intercellular carbon dioxide concentration in leaves. *Australian Journal of Plant Physiology* **9,** 121–137.

Finnigan J.J. (2000) Turbulence in plant canopies. *Annual Review of Fluid Mechanics* **32,** 519–571.

Flanagan L.B. & Ehleringer J.R. (1998) Ecosystem-atmosphere CO_2 exchange: interpreting signals of change using stable isotope ratios. *Trends in Ecology and Evolution* **13,** 10–14.

Flanagan L.B. Brooks J.R. Varney G.T. Berry S.C. & Ehleringer J.R. (1996) Carbon isotope discrimination during photosynthesis and the isotope ratio of respired CO_2 in boreal forest ecosystems. *Global Biogeochemical Cycles* **10,** 629–640.

Francey R.J. Tans P.P. Allison C.E. Enting I.G. White J.W.C. & Trolier M. (1995) Changes in oceanic and terrestrial carbon uptake since 1982. *Nature* **373,** 326–330.

Fung I. Field C.B. Berry J.A., *et al.* (1997) Carbon 13 exchanges between the atmosphere and biosphere. *Global Biogeochemical Cycles* **11,** 507–533.

Garten C.T. & Taylor G.E. Jr (1992) Foliar $\delta^{13}C$ within a temperate deciduous forest: spatial, temporal and species sources of variation. *Oecologia* **90,** 1–7.

Gleixner G., Scrimgeour C., Schmidt H.-L. & Viola R. (1998) Stable isotope distribution in the major metabolites of source and sink organs of *Solanum tuberosum* L. a powerful tool in the study of metabolic partitioning in intact plants. *Planta* **207,** 241–245.

Gu L., Baldocchi D.D., Verma S.B., Black T.A., Vesala T., Falge E.M. & Dowty P.R. (2002) Superiority of diffuse radiation for terrestrial ecosystem productivity. *Journal of Geophysical Research* **107** (D6), DOI 10.1029/2001JD001242.

Hall A.E., Ismail A.M. & Menendez C.M. (1993) Implications for plant breeding of genotypic and drought induced differences in water use efficiency, carbon isotope discrimination and gas exchange. In *Stable Isotopes and Plant Carbon-Water Relations* (eds J.R. Ehleringer, A.E. Hall & G.D. Farquhar) Academic Press, San Diego, CA, USA.

Hanson P.J., S.D.Wullschleger S.A., Bohlman & D.E.Todd. (1993) Seasonal and topographic patterns of forest floor CO_2 efflux from an upland oak forest. *Tree Physiology* **13,** 1–15.

Harley P.C. & Baldocchi D.D. (1995) Scaling carbon dioxide and water vapour exchange from leaf to canopy in a deciduous forest: leaf level parameterization. *Plant, Cell and Environment* **18,** 1146–1156.

Högberg P., Nordgren A., Buchmann N., Taylor A.F.S., Ekblad A., Högberg M.N., Nyberg G., Ottosson-Löfvenius M. & Read D.J. (2001) Large-scale forest girdling shows that current photosynthesis drives soil respiration. *Nature* **411,** 789–792.

Katul G.G. & Albertson J.D. (1999) Modeling CO_2 sources, sinks, and fluxes within a forest canopy. *Journal of Geophysical Research* **104,** 6081–6091.

Keeling C.D. (1958) The concentration and isotopic abundances of atmospheric carbon dioxide in rural areas. *Geochimica et Cosmochimica Acta* **13,** 322–334.

Kruijt B., Lloyd J., Grace J., McIntyre J.A., Farquhar G.D., Miranda A.C. & McCracken P. (1996) Sources and sinks of CO_2 in Rondonian tropical rainforest. In *Amazonian Deforestation and Climate* (eds J.H.C. Gash, C.A. Nobre, J.M. Roberts and R.L. Victoria), pp. 331–351. Wiley and Sons, New York, USA.

Lai C.T., Katul G., Oren R., *et al.* (2000) Modeling CO_2 and water vapor turbulent flux distributions within a forest canopy. *Journal of Geophysical Research* **105,** 26333–26351.

LeRoux X., Bariac T., Sinoquet H., Genty B., Piel C., Mariotti A., Girardin C. & Richard P. (2001) Spatial distribution of leaf water use efficiency and carbon isotope discrimination within an isolated tree crown. *Plant, Cell and Environment* **24,** 1021–1032.

Leuning R. (2000) Estimation of scalar source/sink distributions in plant canopies using Lagrangian dispersion analysis: Corrections for atmospheric stability and comparison with a multilayer canopy model. *Boundary Layer Meteorology* **96,** 293–314.

Lloyd J. & Farquhar G.D. (1994) ^{13}C discrimination during CO_2 assimilation by the terrestrial biosphere. *Oecologia* **99,** 201–215.

Lloyd J., Kruijt B., Hollinger D.Y., *et al.* (1996) Vegetation effects on the isotopic composition of atmospheric CO_2 at local and regional scales: theoretical aspects and a comparison between rain forest in Amazonia and a boreal forest in Siberia. *Australian Journal of Plant Physiology* **23,** 371–399.

Lowdon J.A. & Dyck. W. (1974) Seasonal variations in the isotope ratios of carbon in maple leaves and other plants. *Canadian Journal of Earth Science* **11,** 79–88.

Medina E. & Minchin P. (1980) Stratification of $\delta^{13}C$ values of leaves in Amazonian rain forests. *Oecologia* **45,** 377–378.

Meyers T.P., Hall M.E., Lindberg S.E., *et al.* (1996) Use of the modified Bowen-ratio technique to measure fluxes of trace gases. *Atmospheric Environment* **30,** 3321–3329.

Mortazavi B. & Chanton J.P. (2002) Carbon isotopic discrimination and control of nighttime canopy $\delta^{18}O$-CO_2 in a pine forest in the southeastern United States. *Global Biogeochemical Cycles* in press.

Norman J.M. (1979) Modeling the complete crop canopy. In *Modification of the Aerial Environment of Crops* (eds B.J. Barfield and J.F. Gerber), pp. 249–280. American Society of Agricultural Engineers, St Joseph, MD, USA.

Norman J.M. (1993) Scaling processes between leaf and canopy levels. In *Scaling Processes: Leaf to Globe* (eds J.R. Ehleringer & C.B. Field), pp. 41–76. Academic Press, San Diego, CA, USA.

O'Leary M.H. (1993) Biochemical basis of carbon isotope fractionation. In *Stable Isotopes and Plant Carbon–Water Relations* (eds J.R. Ehleringer, A.E. Hall & G.D. Farquhar), pp. 19–28. Academic Press, San Diego, CA, USA.

O'Leary M.H., Madhavan S. & Paneth P. (1992) Physical and chemical basis of carbon isotope fractionation in plants. *Plant, Cell and Environment* **15,** 1099–1104.

Pataki D., Ehleringer J., Flanagan L., Yakir D., Bowling D., Still C., Buchmann N. & Berry J. (2002) The application and interpretation of Keeling plots in terrestrial carbon cycle research. *Global Biogeochemical Cycles* in press.

Raupach M.R. (1988) Canopy transport processes. In *Flow and Transport in the Natural Environment;* (eds W.L. Steffen & O.T. Denmead). Springer-Verlag, Berlin, Germany.

Raupach M.R. (2001) Inferring biogeochemical sources and sinks from atmospheric concentrations: general consideration and application in vegetation canopies. In *Global Biogeochemical Cycles in the Climate System* (eds E.D. Schulze, M. Heimann, S. Harrison, E. Holland, J. Lloyd, I. Prentice & D. Schimel), pp. 41–60. Academic Press, San Diego, CA, USA.

Raupach M.R., Finnigan J.J. & Bruwet. Y. (1996) Coherent eddies and turbulence in vegetation canopies: the mixing layer analogy. *Boundary Layer Meteorology* **78,** 351–382.

Sage R.F., Wedin D.A. & Li. M. (1999) The biogeography of C_4 photosynthesis: patterns and controlling factors. In *C_4 Plant Biology* (eds R.F. Sage & R.K. Monson), pp. 313–373. Academic Press, San Diego, CA, USA.

Schleser G.H. & Jayasekera R. (1985) $\delta^{13}C$ variations of leaves in forests as an indication of reassimilated CO_2 from the soil. *Oecologia* **65,** 536–542.

Schuepp P.H. (1993) Tansley Review, 59: Leaf boundary layers. *New Phytologist* **125,** 477–507.

Schulze E.D. (1986) Carbon dioxide and water vapour exchange in response to drought in the atmosphere and in the soil. *Annual Review of Plant Physiology* **37,** 247–274.

Sternberg L.S.L.O. (1989) A model to estimate carbon dioxide recycling in forests using $^{13}C/^{12}C$ ratios and concentrations of ambient carbon dioxide. *Agricultural and Forest Meteorology* **48,** 163–173.

Sternberg L.S.L.O., Moreira M.Z., Martinelli L.A., Victoria R.L., Barbosa E.M., Bonates L.C.M. & Nepstad D.C. (1997) Carbon dioxide recycling in two Amazonian tropical forests. *Agricultural and Forest Meteorology* **88,** 259–268.

Tans P.P., Berry J.A. & Keeling R.F. (1993) Oceanic $^{13}C/^{12}C$ observations: a new window on ocean CO_2 uptake. *Global Biogeochemical Cycles* **7,** 353–368.

Thomas D.S., Eamus D. & Bell D. (1999) Optimization theory of stomatal behavior, I. A critical evaluation of five methods of calculation. *Journal of Experimental Botany* **50,** 385–392.

Thomson D.J. (1987) Criteria for the selection of stochastic models of particle trajectories in turbulent flow. *Journal of Fluid Mechanics* **180,** 529–556.

Trolier M., White J.W.C., Tans P.P., Masarie K.A. & Gemery P.A. (1996) Monitoring the isotopic composition of atmospheric CO_2: measurements from the NOAA global air sampling network. *Journal of Geophysical Research* **101,** 25897–25916.

Warland J.S. & Thurtell G.W. (2000) A Lagrangian solution to the relation between a distributed source and concentration profile. *Boundary Layer Meteorology* **96,** 453–471.

Wilson K.B., Baldocchi D.D. & Hanson P.J. (2000) Spatial and seasonal variability of photosynthesis parameters and their relationship to leaf nitrogen in a deciduous forest. *Tree Physiology* **20,** 787–797.

Yakir D. & Sternberg L.S.L.O. (2000) The use of stable isotopes to study ecosystem gas exchange. *Oecologia* **123,** 297–311.

Yakir D. & Wang X.-F. (1996) Fluxes of CO_2 and water between terrestrial vegetation and the atmosphere estimated from isotope measurements. *Nature* **380,** 515–517.

Received 22 April 2002; received in revised form 23 July 2002; accepted for publication 26 July 2002